International Journal of Nanoelectronics and Materials

In Press, Accepted Manuscript – Note to user

Effect of CTAB and $NaBH_4$ Solutions on Ti and Cu Nanoparticles Prepared by Pulsed Laser Ablation

Salma S. Abdullah[1], Sabah A. Salman[2*], and A. Kadhim[3]

[1]Student, Department of Physics, College of Science, University of Diyala, Diyala, Iraq, Diyala General Directorate of Education, Diyala, Email: dr.salmaalshamari@gmail.com
[2]Professor, Department of Physics, College of Science, University of Diyala, Diyala
[3]Professor, Department of Laser and Optoelectronics Engineering, University of Technology, Iraq

Received 22 June 2022, Revised 11 October 2022, Accepted 26 October 2022

ABSTRACT

The effect of different media including cetyltrimethylammonium bromide (CTAB) and sodium borohydride ($NaBH_4$) on the size, shape, optical absorption, and stability of titanium (Ti) and copper (Cu) nanoparticles (NPs) synthesized by laser ablation in liquid was investigated. Ti and Cu NPs were fabricated by irradiating Ti and Cu targets by using a Nd:YAG pulsed laser with a wavelength of 1064 nm, energy of 500 mJ , repetition rate of 1 Hz, and number of pulses of 1000. Results showed the direct effect of the type of surfactant on the size and size distribution of Ti and Cu NP_s under the same laser ablation parameters. Morphological properties were described by field emission scanning electron microscopes (FESEM) images, which revealed the formation of semispherical particles. The EDS results confirmed the spike-induced synthesis of Ti and Cu in CTAB and $NaBH_4$ solutions. The transmission electron microscopy (TEM) images showed the nanostructures of Ti and Cu with spherical particles. The UV-vis absorption spectra showed that the absorption peak of Ti was almost constant at 289 nm, while the peak of Cu disappeared for both solutions. Zeta potential analysis showed that NPs prepared in CTAB solution were more stable than those in $NaBH_4$ solution.

Keywords: Copper Nanoparticles, CTAB**,** Laser Ablation, $NaBH_4$, Titanium Nanoparticles

1. INTRODUCTION

Metal nanoparticles (NPs) have considerable potential because their optical, electronic, and catalytic properties are better than those of bulk materials [1–3]. These properties depend on the size and shape of NPs [4].

Scholars have fabricated NPs by using laser. Creating NPs in a liquid solution through laser ablation is a viable option. Adjusting the laser settings and the conditions of liquid ablation could alter the size and distribution of NPs. Laser ablation is a convenient method for creating NPs because it does not need elaborate equipment, such as vacuum chambers, and hazardous chemicals [5,6]. The size of NPs is one of the parameters that influence their properties, that is, changes in size lead to alterations in properties. According to research, the reactivity of NPs is inversely related to their size [7].

* Corresponding author: dr.salmaalshamari@gmail.com

The particle size changes in response to the viscosity of the liquid ablation environment, and the pressure of the plasma column on the target during ablation changes the size of NPs [8]. A surfactant, which is typically employed as a capping agent, plays a vital function in controlling the stability of NPs as well as their size. Without the surfactant, the interaction between individual particles will be significantly stronger, thereby contributing to the instability of NPs. The molecules of the surfactant are adsorbed on the NP surfaces. During ablation, the use of surfactants to cover NP_s enhances the size uniformity and prevents the particles from coalescing [9].

A close relationship exists between the stability of NPs and the surfactant capping as well as the surface charge of the NPs [10]. Therefore, the stability and size distribution of NPs are greatly dependent on the kind and amount of surfactant used [11]. In solution-based synthesis of colloidal nanocrystals, surfactants are typically used as steric stabilizers and shape controller [12]. CTAB is one of the solutions used to prepare NPs. It has a head that attracts water and is positively charged [8]. CTAB is an important cationic surfactant that is widely used as a steric stabilizer and shape controller for nanocrystals due to its remarkable capability to control the morphology of colloidal nanocrystals. CTAB has been the subject of much research and development in recent years. Recent research indicated that when subjected to hydrothermal conditions, CTAB might encourage the production of metallic Cu NPs on various different metal oxides [12,13]. CTAB consists of the 16-carbon chain as a long tail. As such, this surfactant has amphiphilic properties due to the hydrophilicity of the quaternary ammonium head group and the hydrophobicity of the alkyl tail chain [14,15]. Another surfactant is sodium borohydride, which is used in laser ablation to generate ultrafine NPs. The generated NPs are expected to remain in suspension by the repulsive electrostatic forces between the particles due to the adsorbed borohydride ions [16,17]. Sodium borohydride is cheaper than other ionic surfactants, such as SDS, CTAB, and ethylene glycol.

In this study, CTAB and $NaBH_4$ were used as surfactants to determine how well they could control the size and location of NP_s prepared through laser ablation. In recent years, the preparation of Cu and Ti NPs has become an intensive area of scientific research because Cu NPs exhibit many excellent physical and chemical properties, such as high electrical conductivity and chemical activity.

Cu and Ti NPs are considered possible replacements for Ag and Au particles in some potential applications, such as catalysts and conductive pastes [18]. The current study uses pulsed laser ablation (PLA) to prepare Cu and Ti NP_s in CTAB and $NaBH_4$ solutions.

2. MATERIALS AND METHODS

2.1 Materials

2.1.1 Preparation of Target

The materials used as targets for the ablation process were highly pure Ti and Cu plates, with purity of 98.70% and 98.55%, respectively. The target was cleaned using acetone as solvent and washed with ethanol and distilled water in an ultrasonic bath for 15 minutes to remove organic pollutants. In all the experiments, the level of the solution was 2 mm above the target surface. A Nd:YAG laser with a pulse duration of 10 ns at a 1 Hz repetition rate was used to irradiate the Ti and Cu plates. Figure 1 shows the schematic diagram of the PLAL system.

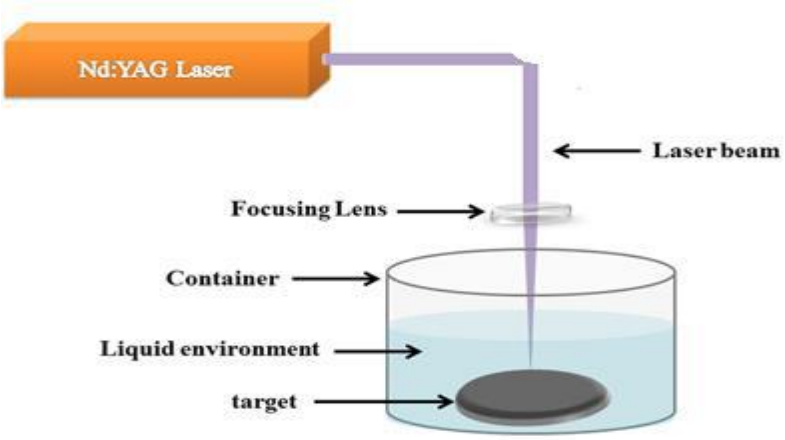

Figure 1 Schematic diagram of PLA system.

2.1.2 Chemical Solution Preparation

CTAB ($C_{19}H_{42}BrN$, MW = 364.45 g/mol, 99.5% purity, Evans UK) was used as a surfactant cationic detergent, and $NaBH_4$ (> 96% purity, MW = 37.83 g/mol, Kanto Chemical Co., Inc.) was used as a stabilizer for mineral colloids. CTAB and $NaBH_4$ will interact with the excised material produced by laser ablation and prevent its accumulation; as such, they will affect the particle size. The solutions of CTAB and $NaBH_4$ were prepared by adding them at concentrations mentioned in Table 1 to 10 mL of DDDW and shaking them carefully. The solution was mixed by a stirrer for 10 minutes to be homogeneous.

Table 1 Parameters of PLA.

Sample Name	Target	Solution	Number Pulses
Ti (1)	Titanium	5 mM CTAB	1000
Ti (2)	Titanium	2 mM $NaBH_4$	1000
Cu(1)	copper	5 mM CTAB	1000
Cu(2)	copper	2 mM $NaBH_4$	1000

2.2 Methods

The morphological characteristics of Ti and Cu NPs were studied by field emission scanning electron microscope (FESEM, ZEISS SIGMAVP, Germany) and transmission electron microscope (TEM, ZEISS LED 912 AB-100KV, Germany). Absorption spectra and surface plasmon resonance (SPR) were recorded for colloids with (UV-vis) spectroscopy type of (Double Beam 1800 UV Spectrometer) manufactured in (Shimadzu, Japan) for the purpose of knowing the effective aggregates. The zeta potential measurement were carried out using Malvern Zeta Sizer (UK).

3. RESULTS AND DISCUSSION

3.1 FESEM Analysis

The morphological structure of Ti and Cu NPs in solutions prepared by PLA was examined using field-emitting scanning electron microscope (FESEM). The average sizes (nm) of Ti and Cu NPs prepared by PLA are shown in Table (2). Figure (1) illustrates the FESEM images and the diameter distribution of NPs prepared in 5 mM CTAB and 2 mM $NaBH_4$ for Ti and Cu, respectively. The Ti and Cu particles obtained were within the nanoscale and had semispherical shapes.

Table 2 Average sizes (nm) of Ti and Cu NPs.

Nanoparticle Types	Solvent	Average Size (nm)
Ti NPs	5 mM CTAB	29.523
	2 mM $NaBH_4$	35.067
Cu NPs	5 mM CTAB	40.791
	2 mM $NaBH_4$	37.89

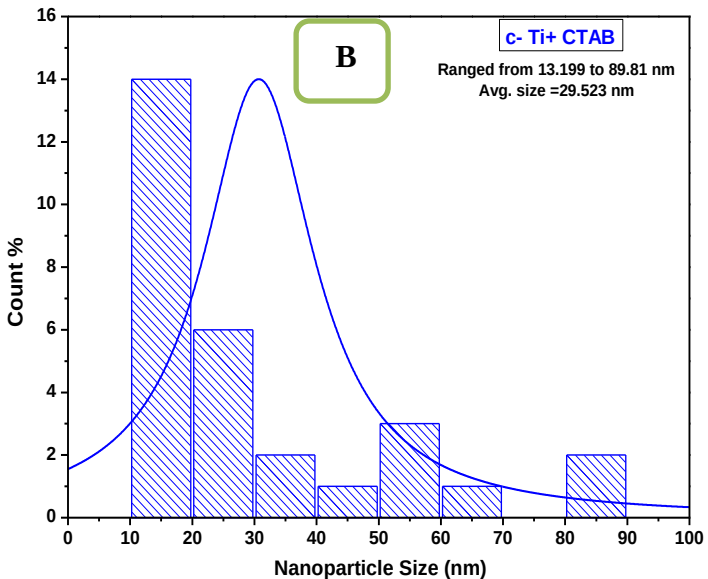

International Journal of Nanoelectronics and Materials

In Press, Accepted Manuscript – Note to user

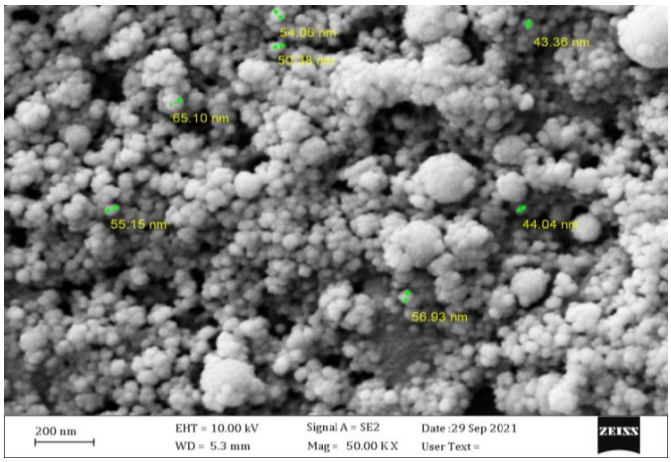

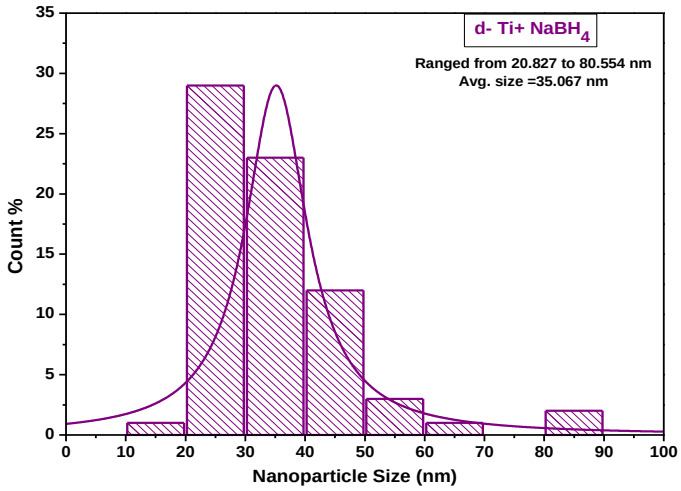

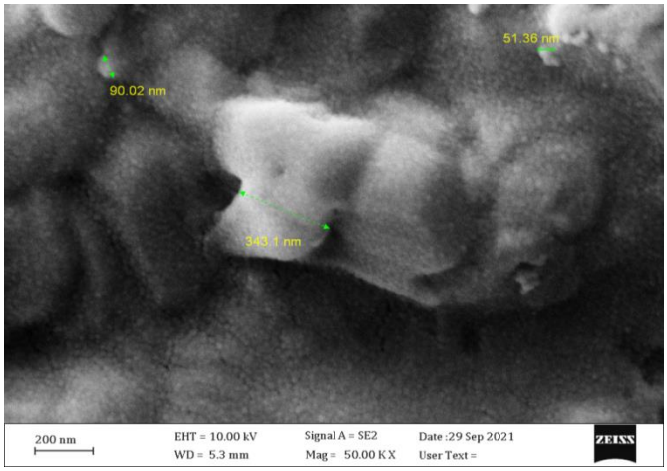

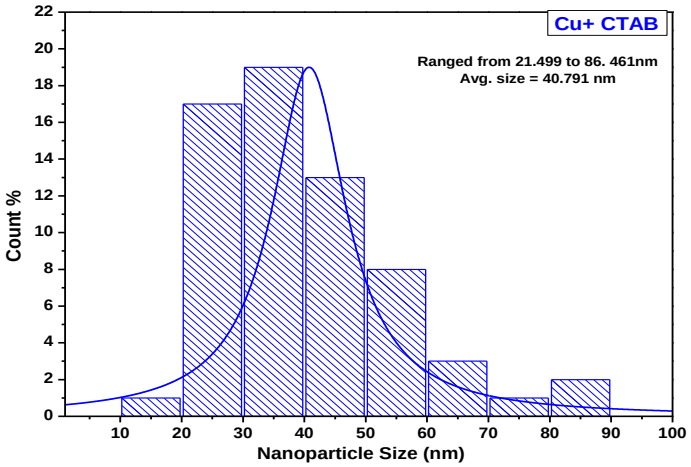

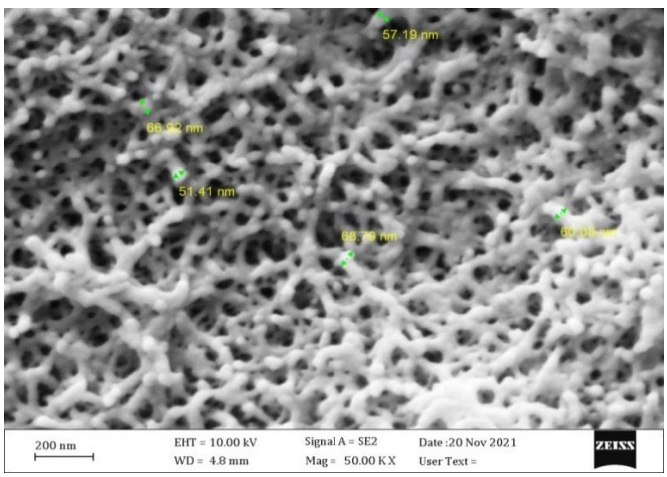

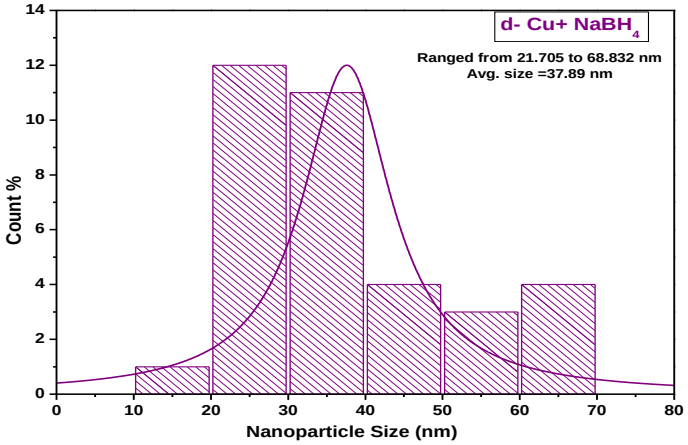

Figure 2. FESEM image of colloidal Ti and Cu NPs.
A- FESEM images of Ti and Cu NPs at 200 nm.
B- Diameter distribution of the prepared Ti and Cu NPs.

3.2 EDS Analysis

Figure (2) shows the EDS diagram for each sample prepared in CTAB and $NaBH_4$ solutions. In the presence of other elements such as Na, Si, and V, the appearance of some elements is due to the components of the used plates and the quartz base substrate on which they were deposited [19].

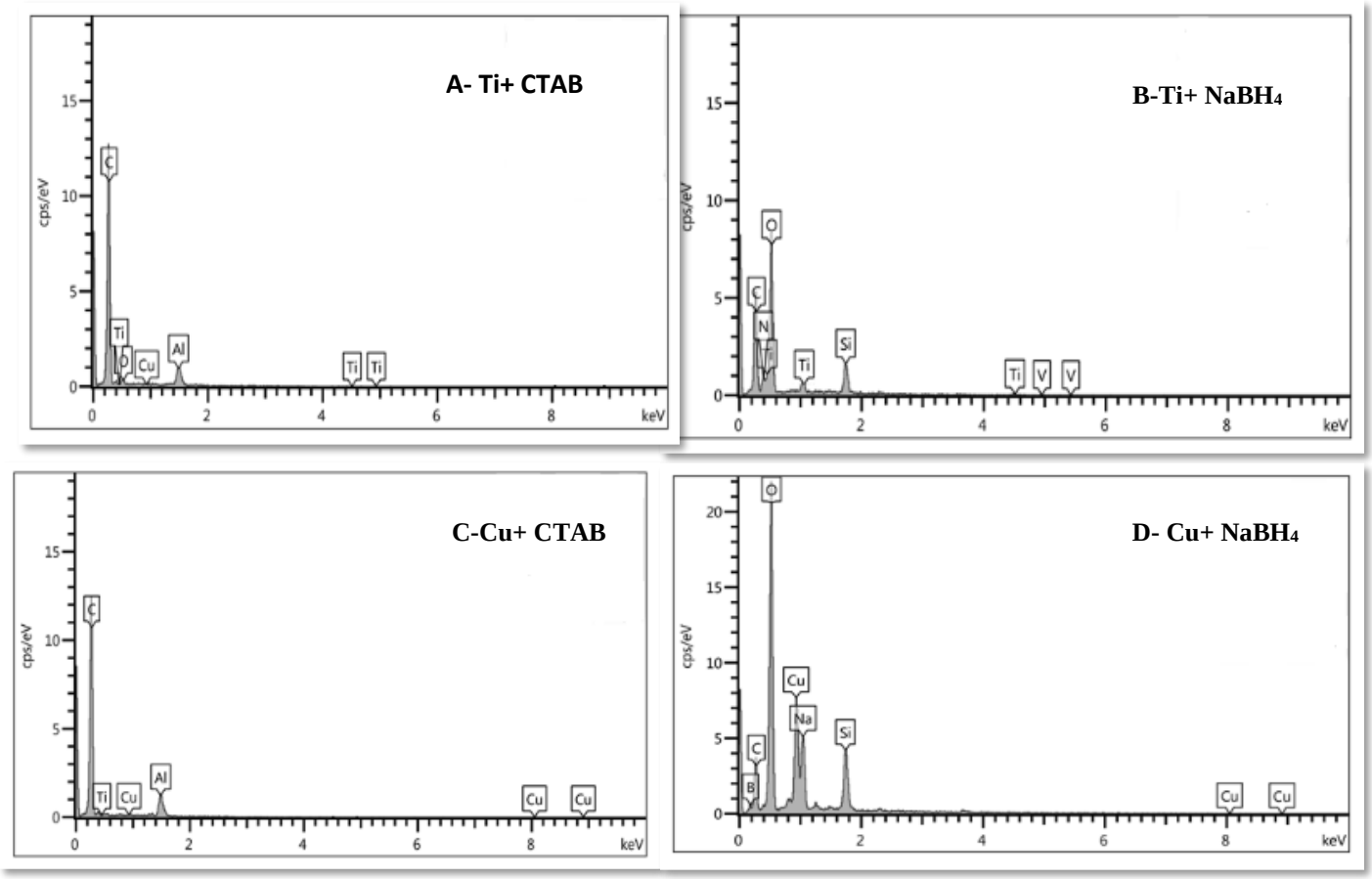

Figure 3. Spectrum from EDS analysis.
A- Highest peak for carbon at 0.13 KeV, followed by aluminum at 0.25 KeV and titanium at 0.22 KeV. B - Highest peak for oxygen at 0.25 KeV, followed by carbon at 0.13 KeV and Ti at 1.1 KeV. C- Highest peak for carbon at 0.15 KeV, followed by aluminum at 1.5 KeV and copper at 0.9 KeV. D- Highest peak for oxygen at 0.25 KeV followed by copper at 0.92 KeV.

3.3 TEM Analysis

Spherical NPs of Ti and Cu in CTAB and $NaBH_4$ solutions were successfully synthesized through the mechanism of ablation in PLA. TEM analysis was conducted to determine surface morphology and size distribution. According to our observations, the surfactants reduced the size of NPs.

This finding can be explained by understanding the mechanism of generating NPs during laser ablation in the liquid with a nanosecond laser. NPs are formed in plume, where plasma plume species are nucleated by collisional sticking and aggregation due to the condensation and cooling of the plume, resulting in adiabatic expansion. The particles are then dispersed into the liquid medium to serve as nucleation centers for the incoming NP species via diffusion. After the cavitation bubbles collapse, further NP growth can occur. Hence, if surfactants exist in the solution, then they can adsorb and cover existing NPs to prevent further NP growth [20]. Figure (3) shows the TEM images of colloidal Ti and Cu NPs.

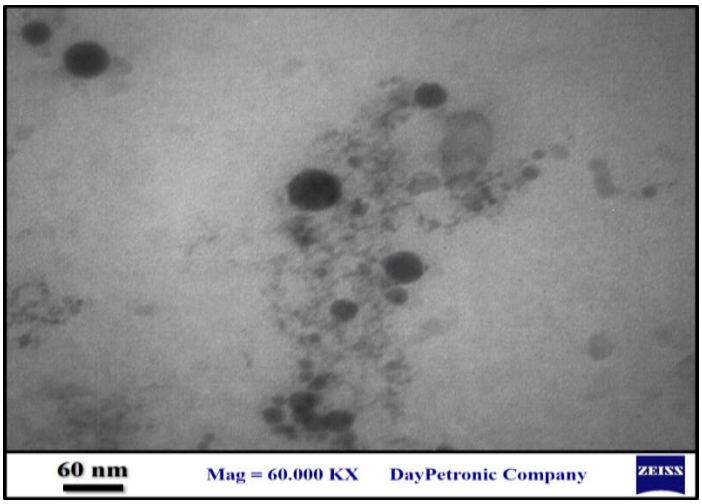

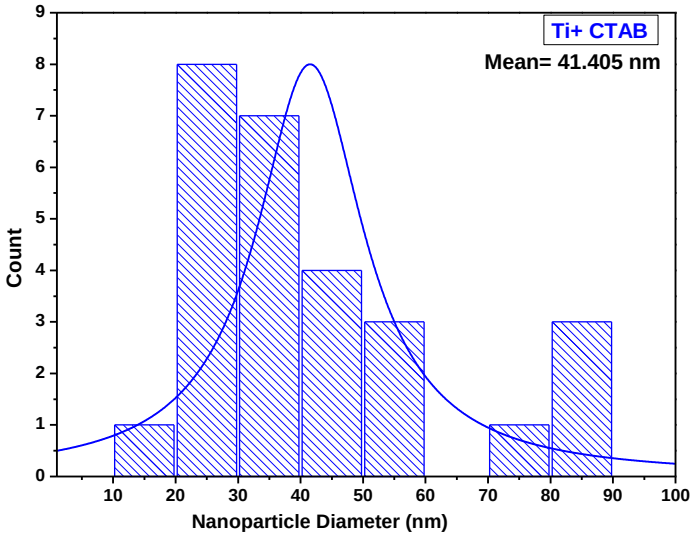

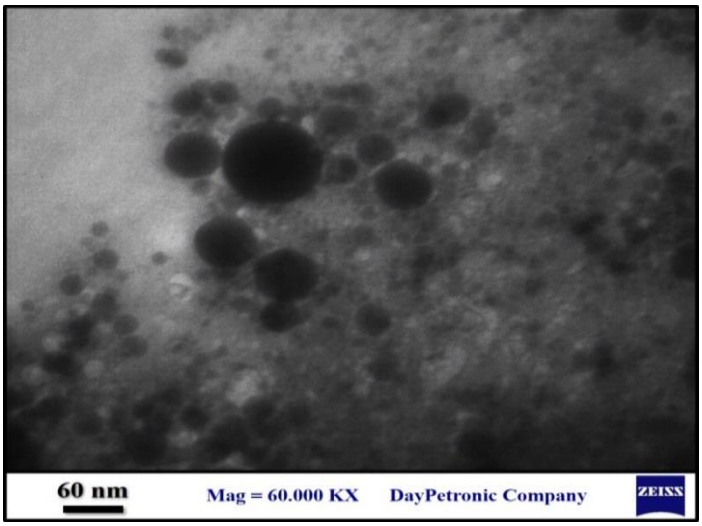

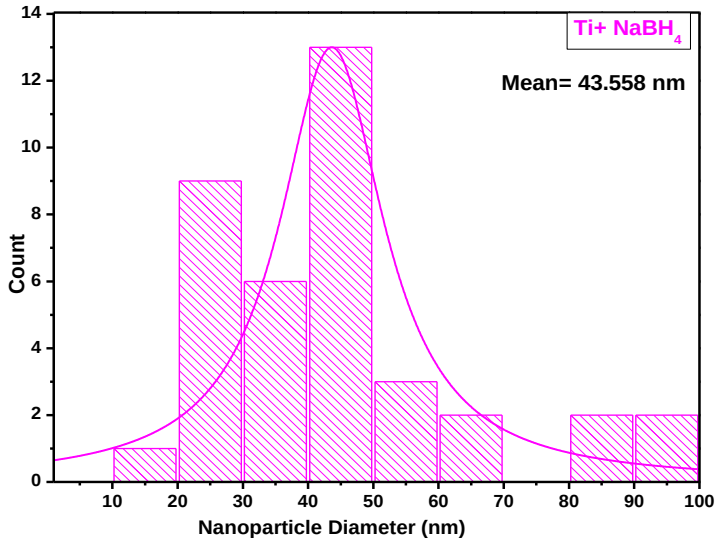

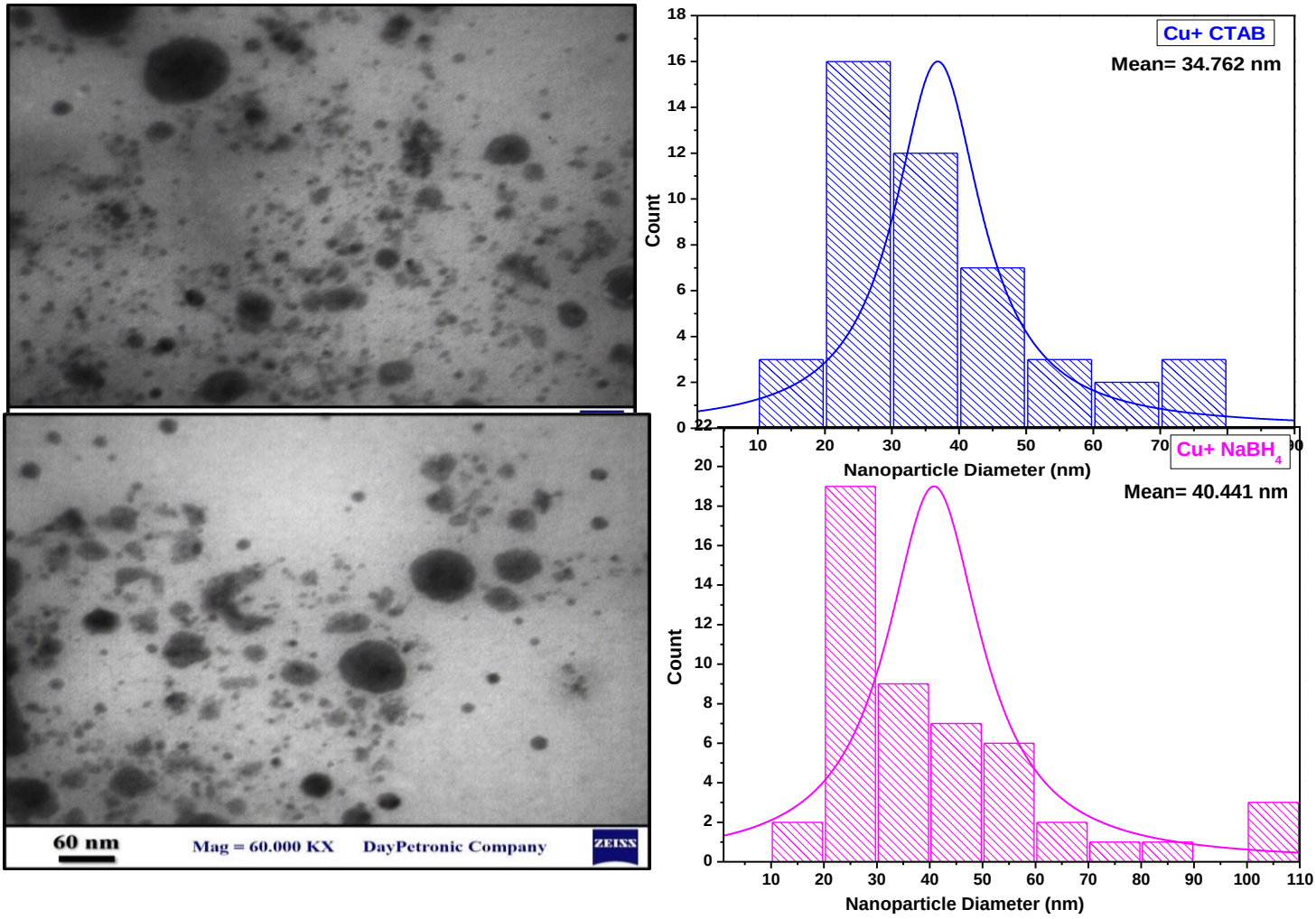

Figure 4. TEM images of colloidal Ti and Cu NPs

3.4 UV-vis Analysis and Energy Gap Calculation

The absorption spectra of the prepared colloidal solutions were studied using UV-vis as the laser beam falls on the surface of the metal immersed in the liquid, causing a spark column with a strong shock wave that spreads in all directions. A visible cloud of metal particles then emerges from the metal surface and floats in all directions in the liquid. When the number of laser pulses was increased, the color of the solution changed and its intensity increased, indicating the formation of a solution containing metallic NPs of the extracted metal. Surface plasmon resonance (SPR) peaks in the visible and ultraviolet regions are a distinct indication of the formation of metal NPs [21].

The absorbance and energy gap values for NPs generated from CTAB and $NaBH_4$ solutions are shown in Table (3). Figure (4) shows the UV-vis absorption spectra of colloidal Ti NPs, which were approximately constant at 289 nm. As shown in Figure (5), the absorbance spectrum of the solution of copper NPs was obtained by laser ablation of a copper plate in CTAB and $NaBH_4$ solutions.

The intensity of the peaks decreased due to the accumulation and agglomeration of NPs, so their weight increased and they submerged to the bottom of the solution. After a while, the SPR peak disappeared.

Figures (6) and (7) show the direct band gap estimates for colloidal Ti and Cu NPs. Optical energy gap was calculated using Tauc's formula, where the energy gap values are within 3.30–3.10 eV for Ti NPs and 2.84–2.95 eV for Cu NPs in CTAB and $NaBH_4$ solutions. The increase in Eg could be attributed to levels near the electron-filled conduction band, so the electrons requires more energy to move. This phenomenon occurs if the energy gap increases [22].

Table 3 Absorption, surface plasmon resonance, and energy gap values of Ti and Cu NPs.

Nanoparticle Types	Solvent	Absorbance (a.u)	Surface Plasmon Resonance SPR (nm)	E_g (eV)
Ti NPs	5 mM CTAB	0.45	289	3.30
	2 mM $NaBH_4$	1.38	289	3.21
Cu NPs	5 mM CTAB	0.16	---------	2.84
	2 mM $NaBH_4$	0.12	----------	2.95

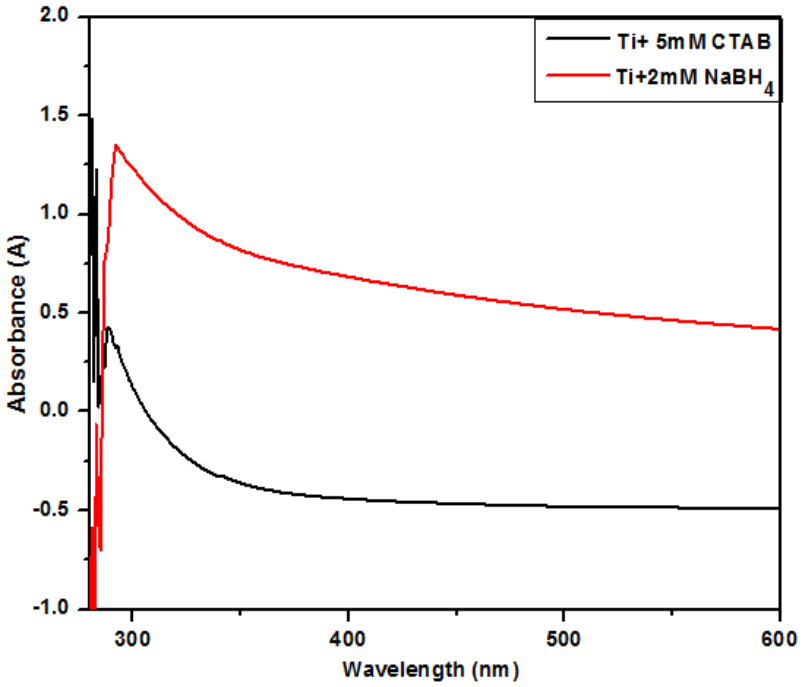

Figure 5. UV-visible absorption spectra of colloidal Ti NPs.

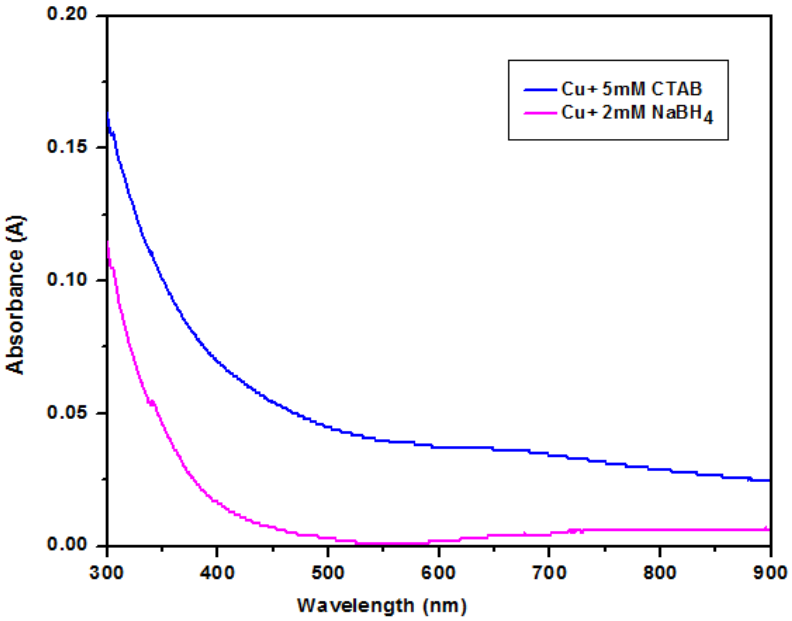

Figure 6. UV-visible absorption spectra of colloidal Cu NPs.

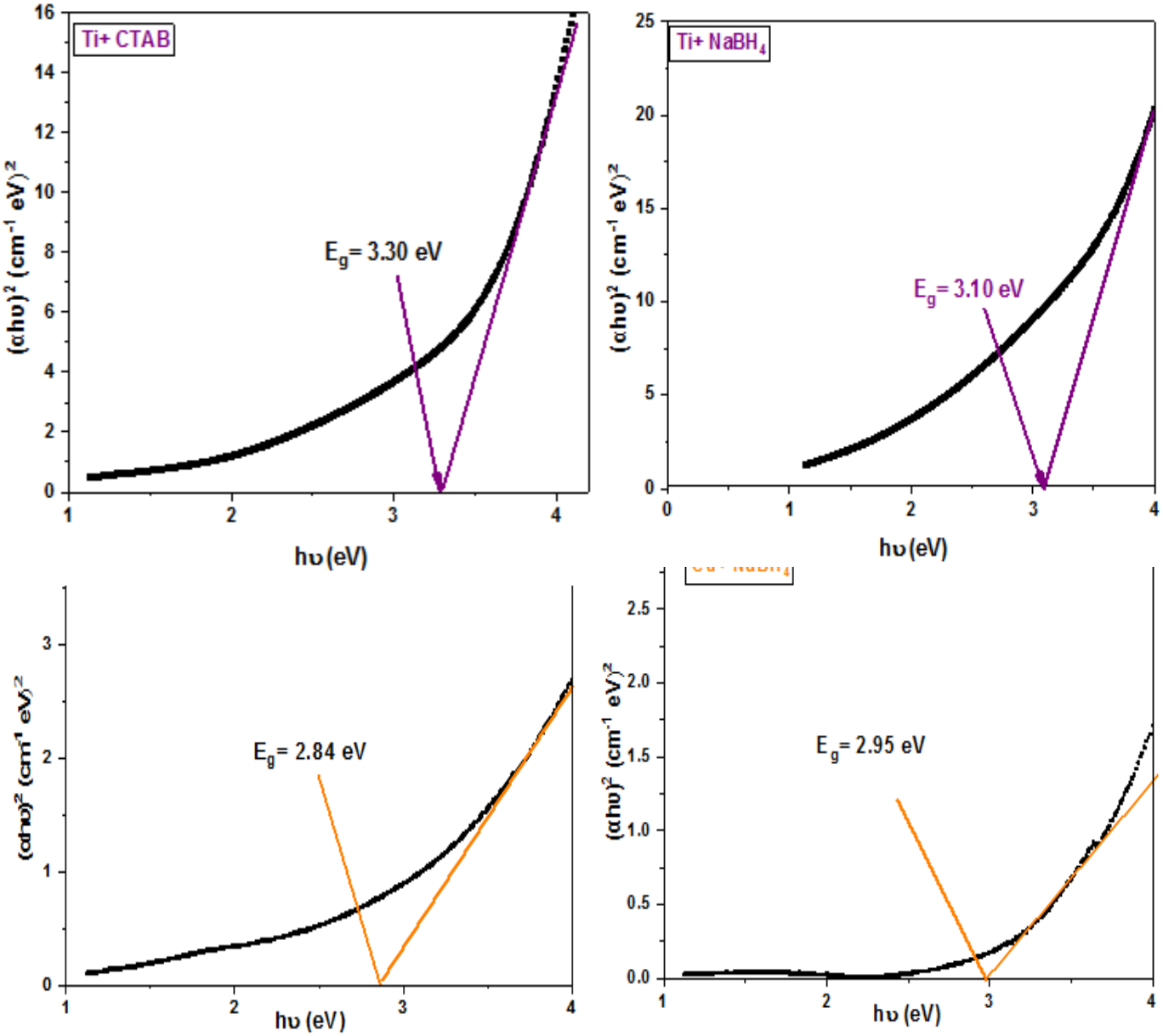

Figure 8. Direct band gap estimations of colloidal Cu NPs.

3.5 Zeta Potential Analysis

Zeta potential was measured to evaluate the stability of the materials used and prepared by PLA and determine the presence of agglomeration in the solutions. Zeta potential values higher than +30 mV to lower than -30 mV indicate the stability of NPs [23].

The zeta potential values of Ti and Cu NPs are shown in Table (4). Figure (8) shows the zeta potential distribution of Ti and Cu NPs illuminated by 1064 nm wavelength for different types of surfactant solutions. The zeta values are 47.5–5.10 mV for Ti NPs and 15.5–3.10 mV for Cu NPs in CTAB and $NaBH_4$ solutions.

Table 4 Zeta potential values of Ti and Cu NPs.

Solutions	Zeta Potential (mV)
Ti+ 5 mM CTAB	47.5 mV
Ti+ 2 mM $NaBH_4$	-5.10 mV
Cu+ 5 mM CTAB	15.5 mV
Cu+ 2 mM $NaBH_4$	-3.10 mV

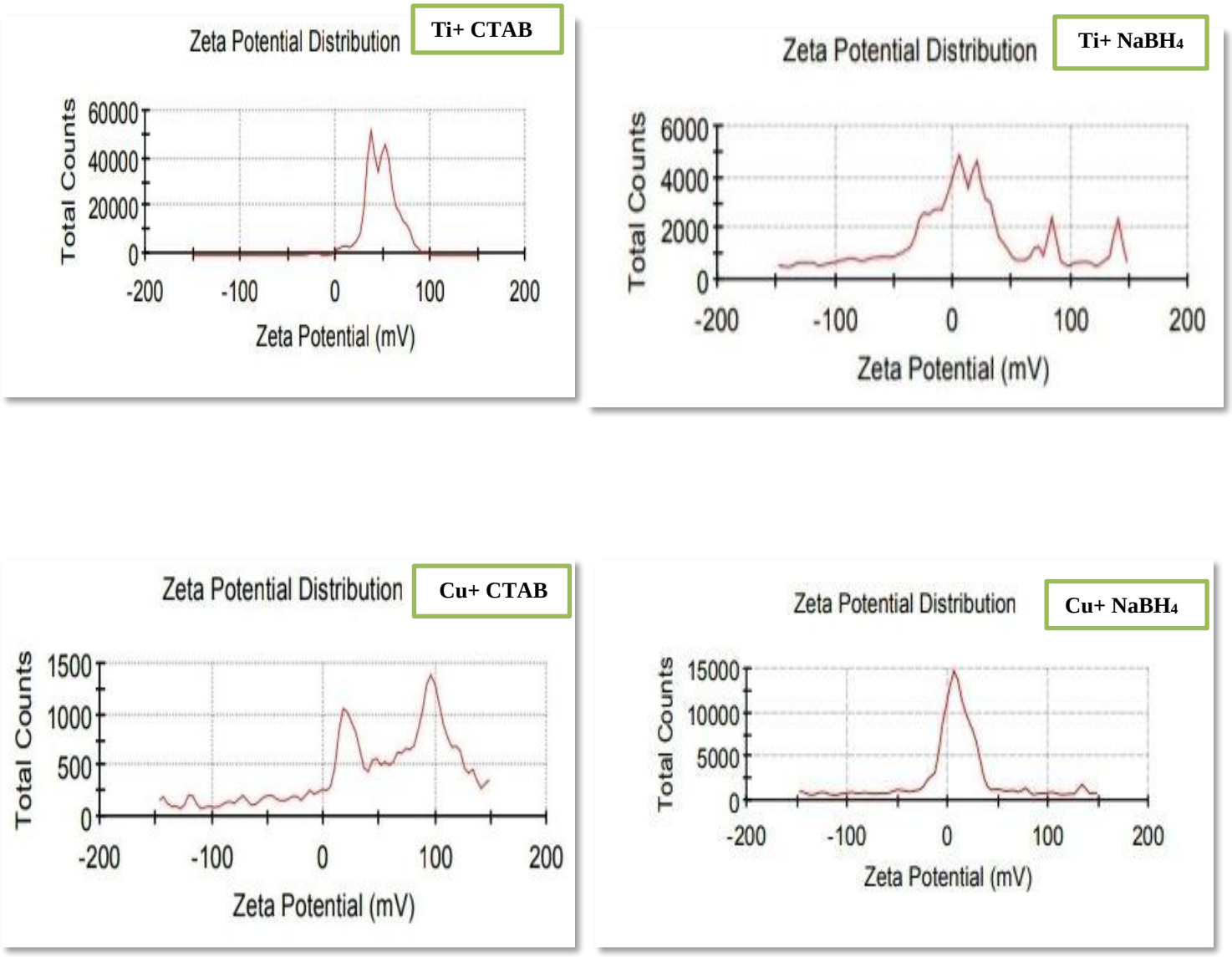

Figure 9. Zeta potential distribution of Ti and Cu nanoparticles in two solutions

4. CONCLUSION

In this study, Ti and Cu NPs were synthesized using CTAB and $NaBH_4$ solutions through nanosecond PLA. FESEM and TEM measurements were conducted to detect NPs with size less than 50 nm. The energy gap values were 3.30–3.310 eV for Ti NPs and 2.84–2.95 eV for Cu NPs in CTAB and $NaBH_4$ solutions. The increase in the energy gap of colloidal Ti and Cu NPs could be due to the decreased size of the ablated particles as a result of the quantum size effect. For potentiometric analysis, the zeta

potential of NPs prepared in CTAB was more stable than that in $NaBH_4$ because CTAB is a cationic solution.

REFERENCES

[1] Medynska, A. Z., Marchelek, M., Diak M., and Grabowska, E., Noble metalbased bimetallic nanoparticles: the effect of the structure on the optical, catalytic and photocatalytic properties, Advances in Colloid and Interface Science, **229** (2016) pp. 80–107.

[2] Fan, Z. and Zhang, H., Crystal phase-controlled synthesis, properties and applications of noble metal nanomaterials, Chemical Society Reviews, **45** (2016) pp. 63–82.

[3] Rai, M. , Ingle, A. P., Gupta, I. and Brandelli, A., Bioactivity of noble metal nanoparticles decorated with biopolymers and their application in drug delivery , International Journal of Pharmaceutics, **496** (2015) pp. 159–172.

[4]. Kelly, K. L, Coronado, E. , Zhao L. L. and Schatz, G. C., The optical properties of metal nanoparticles: the influence of size, shape and dielectric environment, Journal of Physical Chemistry B, 107 (2003) pp. 668–677.

[5] He, C., Sasaki, T., Zhou, Y. , Shimizu, Y., Masuda, M. and Koshizaki, N., Surfactant assisted preparation of novel layered silver bromide-based inorganic/organic nanosheets by pulsed laser ablation in aqueous media, Advanced Functional Materials, **17** (2007) pp. 3554–3561.

[6] Ishikawa, Y., Shimizu, Y., Sasaki, T. and Koshizaki, N., Preparation of zinc oxide nanorods using pulsed laser ablation in water media at high temperature, Journal of Colloid and Interface Science, **300** (2006) pp. 612–615.

[7] Ramakrishna, G. and Ghosh, H. N., Effect of particle size on the reactivity of quantum size ZnO nanoparticles and charge-transfer dynamics with adsorbed catechols, Langmuir, **19** (2003) pp. 3006–3012.

[8] Moradi, M., Solati, E., Darvishi, S. and Dorranian, D., Effect of aqueous ablation environment on the characteristics of ZnO nanoparticles produced by laser ablation, Journal of Cluster Science, **27** (2016) pp. 127–138.

[9]Chua, M.J. and Murakami, Y. Influence of surfactants and dissolved gases on the silver nanoparticle plasmon resonance absorption spectra formed by the laser ablation processes, ISRN Physical Chemistry, **2013** (2013) pp. 1-7.

[10] Zulfajri, M., Huang, W., Huang, G. and Chen, H. F., Effects of different surfactant charges on the formation of gold nanoparticles by the LASiS method, Materials, **14** (2021) pp.1-13.

[11] Ishida, Y., Akita, I., Sumi, T., Matsubara, M. and Yonezawa, T., Thiolate-protected gold nanoparticles via physical approach: Unusual structural and photophysical characteristics, Scientific Reports, **6** (2016) pp.1-14.

[12] Zamiranvari, A., Solati, E. and Dorranian, D., Effect of CTAB concentration on the properties of graphene nanosheet produced by laser ablation, Optics and Laser Technology, **97** (2017) pp. 209–218.

[13] Tada, M., Bal, R., Namba, S., Y. Iwasawa, Surface-promoted novel synthesis of supported metallic Cu nanoparticles active for selective dehydrogenation of methanol, Applied Catalysis A: General, **307** (2006) pp. 78–84.

[14] Bahri, M. A. , Hoebeke, M., Grammenos, A., Delanaye, L., Vandewalle, N. and Seret, A., Investigation of SDS, DTAB and CTAB micelle microviscosities by electron spin resonance, Colloids and Surfaces A: Physicochemical and Engineering Aspects, **290** (2006) pp. 206-212.

[15] Lim, J., Lee, N., Lee, E. and Yoon, S., Surface modification of citrate-capped gold nanoparticles using CTAB micelles, Bulletin of the Korean Chemical Society, **35** (2014) pp. 2567-2569.

[16] Dong, P. V., Ha, C. H., Binh, L. T. and Kasbohm, J., Chemical synthesis and antibacterial activity of novel-shaped silver nanoparticles, International Nano Letters, **2** (2012) pp. 1-9.

[17] Mulfinger, L., Solomon, S. D., Bahadory, M., Jeyarajasingam, A. V., Rutkowsky, S. A. and Boritz, C., Synthesis and study of silver nanoparticle, Journal of Chemical Education, **84** (2007) pp. 322-325.

[18] Qing-ming, L., De-bi, Z., Yamamoto, Y., Ichin, R. and Okido, M., Preparation of Cu nanoparticles with $NaBH_4$ by aqueous reduction method, Transactions of Nonferrous Metals Society of China, **22**(2012) pp. 117-123

[19] Salim, A. A., Bidin, N., Bakhtiar, H., Ghoshal, S. K., Al Azawi, M. and Krishnan, G., Optical and structure characterization of cinnamon nanoparticles synthesized by pulse laser ablation in liquid (PLAL), International Laser Technology and Optics, Journal of Physics: Conf. Series , 1027 (2018).

[20] Semaltianos, N. G., Nanoparticles by laser ablation, Critical Reviews in Solid State and Materials Sciences, **35** (2010) pp. 105-124.

[21] Mejia, O. O., Camacho, M. A., Cardoso, O. O., Castanares, R. L. and Nestor, A. R. V., Silver nanoparticles obtained by laser ablation using different stabilizers, Japanese Journal of Applied Physics, **52** (2013) pp. 1-6.

[22] Rashed, H. H. and Moatasemballah, J., Synthesis and characterization of Au:CuO nanocomposite by laser soldering on porous silicon for photodetector, Journal of Al-Nahrain University, **20** (2017) pp. 49-59.

[23] Alnassar, S. I., Akman, E., Oztoprak, B. G., Kacar, E., Gundogdu, O., Khaleel, A. and Demir, A. , Study of the fragmentation phenomena of TiO_2 nanoparticles produced by femtosecond laser ablation in aqueous media", Optics & Laser Technology, Vol. 51, (2013) pp.17–23.